Project funded by the European Commission under the 6th (EC) RTD Framework Programme (2002- 2006) within the framework of the specific research and technological development programme “Integrating and strengthening the European Research Area”

**Project UpWind**

Contract No.:
019945 (SES6)

“Integrated Wind Turbine Design”

# WP6: Remote Sensing
# D6.15.1 An approach to power curve with lidar in complex terrain



| | |
|---|---|
| AUTHOR: | Paula Gómez Arranz |
| AFFILIATION: | Fundación CENER-Ciemat |
| ADDRESS: | C/ Ciudad de la Innovación. 31621 Sarriguren. Navarra. Spain |
| TEL.: | +34 948 25 28 00 |
| EMAIL: | pgomez@cener.com |
| FURTHER AUTHORS: | |
| REVIEWER: | |
| APPROVER: | |



*Document Information*

| | |
|---|---|
| DOCUMENT TYPE | Final Report |
| DOCUMENT NAME: | CENER-D6.15.1-final.pdf |
| REVISION: | |
| REV.DATE: | February 2011 |
| CLASSIFICATION: | R0: General public |
| STATUS: | |

**Abstract:** This document presents the results of a measurement campaign in complex terrain performed by CENER using a lidar and an instrumented met mast in front of a wind turbine. The aim is to perform a first approach to power curve with lidar in complex terrain.

# Contents



| STATUS, CONFIDENTIALITY AND ACCESSIBILITY | | | | | | | | | | |
|---|---|---|---|---|---|---|---|---|---|---|
| **Status** | | | | **Confidentiality** | | | | **Accessibility** | | |
| **S0** | Approved/Released | | | **R0** | General public | **x** | | Private web site | | |
| **S1** | Reviewed | | | **R1** | Restricted to project members | | | Public web site | | |
| **S2** | Pending for review | | | **R2** | Restricted to European. Commission | | | Paper copy | | |
| **S3** | Draft for commends | | | **R3** | Restricted to WP members + PL | | | | | |
| **S4** | Under preparation | | | **R4** | Restricted to Task members +WPL+PL | | | | | |

**PL:** *Project leader* **WPL:** *Work package leader* **TL:** *Task leader*

# 1. Introduction

CENER's second contribution to work package 6, task 6.6, consists of a measurement campaign in complex terrain, in which a ZephIR lidar is installed close to a meteorological mast and in the vicinity of a wind turbine. The goal is to perform the power curve performance measurement of a multi-megawatt wind turbine according to IEC 61400-12-1 in complex terrain, in which additionally a lidar is located in the vicinity of the reference meteorological mast.

The wind profile information provided by the lidar is used to investigate the effect of wind shear on the standard power curve. Secondly, in an attempt to reduce the influence of the wind profile on the power curve, the wind speeds provided by the lidar at different heights are used to obtain an equivalent wind speed, weighted across the rotor swept area, which is used as the reference wind speed of the power curve.

Since the measurement takes place in complex terrain, this raises the subject of how to correlate the wind profile at the turbine position and the wind profile measured by the lidar; for this matter different approaches are presented in this report.

The power curve measurement with lidar that is described in this report took place between 22/4/2009 and 2/8/2009. The lidar was deployed in this location prior to the beginning of that period for the aim of performing lidar to mast comparisons for task 6.6. The results of that comparison are summarized in deliverable D6.6.2 [1]. The reasons for the delay from the original time schedule are detailed in that report (start-up date of the measurement campaign postponed due to delay of grid connection permits of the wind farm where the measurement takes place, and failure of lidar unit).

Some preliminary results of the power curve measurement with lidar in complex terrain were presented in CENER's summaries of activities in months 42 and 52. This document is the final report corresponding to deliverable D6.15.1.

# 2. Motivation

The current power curve verification standard [2] requires the measurement of turbine electrical power and wind speed at hub height. However, variations in wind shear may affect the power output of a wind turbine. In such cases, the wind speed at hub height is not representative enough of the wind conditions across the whole rotor area. In this context, remote sensing devices can be a useful tool to measure the wind profile within the rotor swept area.

The standard is currently undergoing a revision which aims, among others, at accounting for the influence of wind shear on the power curve uncertainty and at developing a procedure that uses wind speed profile information to reduce the sensitivity of the power curve due to shear. In this context, extensive work has been carried out by WP6 colleagues in the development of a methodology for power performance measurements using an "equivalent wind speed" definition (obtained from wind profile measurements), which significantly reduces the scatter due to shear in the power curve [3].

The aim of this work is to make an approach to the application of the equivalent wind speed method using a lidar (to measure the wind speed profile), in a power performance measurement in complex terrain. The objective is to check if the use of the equivalent wind speed definition can lead to a power curve with less scatter than the standard power curve.

It is important to mention that in this case the application of the equivalent wind speed method is complicated by not having a precise correlation between the wind profiles at the lidar position and at the wind turbine position.

# 3. Test site description

The test site is a wind farm in complex terrain, located in Albacete, Spain. The test area consists of hills covered with low forest, and several rows of wind turbines, as seen in Figure 1. The terrain is fairly irregular in all directions (Figure 2). The prevailing wind direction is West, and the secondary is South.

For the sake of confidentiality, no information about the wind turbine under test is given in this report. Suffice it to say, for the purpose of this study, that it is a multi-megawatt wind turbine (see Figure 3). For the same reason, the graphs included in this report are presented in dimensionless units. This means that power values are divided by one constant reference value of power ($P_{nom}$, which is the wind turbine rated or "nominal" power), and wind speeds are divided by one constant reference value of wind speed ($U_{nom}$, which is the wind turbine rated or "nominal" wind speed).

**Figure 1:** *General view of the wind farm where the test takes place.*

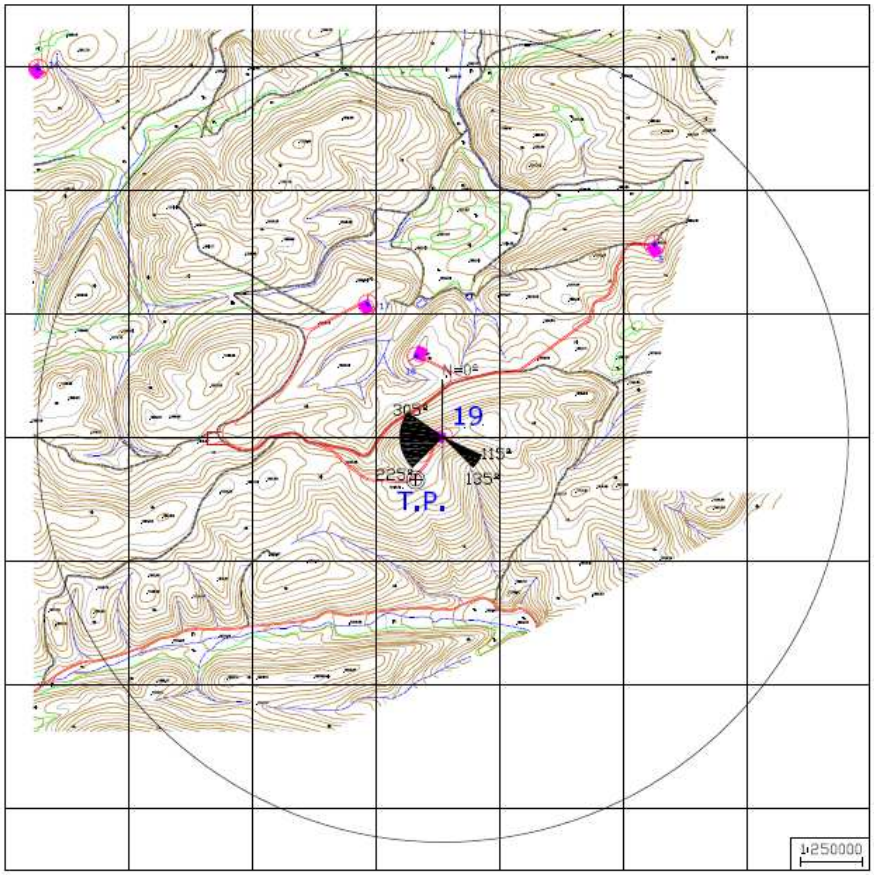


**Figure 2:** *Topographic map (5m-contour-lines) of the test site, including the final measurement sector (see section 5) of the power performance measurement. Wind turbine under test is labelled "19" and reference meteorological mast is labelled "T.P.". Altitude of the reference mast base is 1300m a.s.l.*

The reference mast is installed at a distance of 2.5D from the wind turbine (D is the rotor diameter of the wind turbine), and at an angle of -148º from it.

An assessment of obstacles is performed according to [2, Annex A], in order to indentify the measurement sector where both the mast and the wind turbine are free from flow distortion due to wakes form the neighbouring wind turbines or other significant obstacles. In this case, the only obstacles considered relevant are the wind turbines of the wind farm. The resulting non-perturbed sector is [70º,305º).

The test site is assessed for sources of wind flow distortion due to topographical variations, according to [2, Annex B] for the given free measurement sector. The result is that the terrain doesn't fulfil the requirements to be considered flat terrain, and as a consequence a site calibration is performed prior to the power curve measurement.

**Figure 3:** *Wind turbine under test and reference mast used in the power performance measurement.*

# 4. Description of equipment

Concerning the instrumentation listed in 4.1, 4.2 and 4.4, the pressure sensor, the temperature and humidity sensor, the propellers, the data acquisition system and the power transducers have been calibrated by laboratories accredited by UNE-EN ISO/IEC 17025 standard [4]. Additionally, cup anemometers have been calibrated by a laboratory accredited by Measnet [5]. The procedure in [2, Annex K] is followed to check that the main (top-mounted) cup anemometers maintain their calibration during the measurement period. Cup anemometers are of class B 2.9-3.8 according to [6].

## 4.1 Reference mast

The reference mast instrumentation consists of a top-mounted cup anemometer and additional sensors distributed along the mast, as detailed in Table 1. This table includes only the instrumentation present during both the site calibration and the power curve measurement stages. During some part of the power curve phase, additional sensors (sonic anemometers) were installed on the mast, for the purpose of the lidar to meteorological mast correlations described in [1].

| Sensor | Height a.g.l. | Model | Boom orientation |
|---|---|---|---|
| Main cup anemometer | $H_{HUB}$ | Thies First Class | - |
| Cup anemometer | $H_{HUB}$ – 2m | Thies First Class | 195º |
| Wind Vane | $H_{HUB}$ – 2m | Thies-Compact | 15º |
| Propeller | $H_{HUB}$ – 5m | Young 27106T-Y | 15º |
| Humidity & Temperature sensor | $H_{HUB}$ – 5m | Ammonit –P6831 | - |
| Cup anemometer | $0.5H_{HUB}$ | Thies First Class | 195º |
| Wind Vane | $0.5H_{HUB}$ | Thies-Compact | 15º |
| Pressure sensor | 1.5m | Vaisala-PTB100A | - |
| Rain sensor | 1.5m | Lambrecht | - |

**Table 1:** *Reference mast instrumentation during the site calibration and power curve phases. Sensor height is indicated by meters above ground level, or relative to the wind turbine hub height ($H_{HUB}$).*

## 4.2 Calibration mast

The "calibration" mast is the temporary mast located at the wind turbine position, during the site calibration stage. It has a top-mounted cup anemometer and additional sensors, detailed in the following table:

| Sensor | Height a.g.l. | Model | Boom orientation |
|---|---|---|---|
| Main cup anemometer | $H_{HUB}$ | Thies First Class | - |
| Cup anemometer | $H_{HUB}$ – 2m | Thies First Class | 195º |
| Wind Vane | $H_{HUB}$ – 2m | Thies-Compact | 15º |
| Propeller | $H_{HUB}$ – 5m | Young 27106T-Y | 15º |

**Table 2:** *Calibration mast instrumentation. Sensor height is indicated by meters above ground level, or relative to the wind turbine hub height ($H_{HUB}$).*

## 4.3 Lidar

The lidar is a ZephIR, which is configured to measure at heights $0.5H_{HUB}$, $0.73H_{HUB}$, $0.83H_{HUB}$, $H_{HUB}$ and $1.25H_{HUB}$. The heights ranging from $0.5H_{HUB}$ to $H_{HUB}$ are selected to match instrumented levels in the mast and allow for the comparison between lidar and mast instruments for the purposes of [1], simultaneously to the present power performance measurement. The additional height of $1.25H_{HUB}$ is selected for the purpose of the present report.

Two additional heights are sensed (as a factory setting), 38m and 800m, which are used only by the ZephIR internal cloud correction software to process wind data in order to compensate for cloud effects. The version of the cloud correction algorithm was the latest developed up to that date. Scan settings are modified from the factory default three-second scan per height to one-second scan per height. The lidar was only present during the power curve phase.

### 4.4 Other equipment

A data acquisition system is installed at the base of the reference mast, in order to collect data from the sensors of the calibration mast and the reference mast during the site calibration phase; and wind turbine data and meteorological data from the reference mast during the power curve phase.

Power transducers are installed inside the wind turbine, which comply with the class requirements indicated in [2].

## 5. Site Calibration

Due to terrain effects or obstacles, the wind speed at the wind turbine position and at the reference mast positions may be significantly different. The reference standard requires a site calibration in complex terrains, in order to obtain a set of "flow correction factors", $\alpha_j$, (ratio between the wind speed at hub height at the wind turbine position and the wind speed at hub height at the reference mast) for all the wind directions ("j") in the measurement sector. These factors are used during the power curve measurement, to correct for flow distortion the reference wind speed (wind speed measured by the cup anemometer mounted at hub height in the reference mast).

**Figure 4:** *Calibration mast (left) and reference mast (right) during site calibration.*

The site calibration is performed from 15/11/2007 to 4/3/2008. During this period the lidar was not present in the test site, since it was not available for this project at that moment.

The fact that there is not sufficient profile information from site calibration imposes an important constraint on this study. As mentioned earlier, for the correct application of the equivalent wind speed method it would be necessary to perform wind speed profile measurements during site calibration in order to: 1) check if there are significant changes between the profiles at the reference mast position and at the calibration mast position; 2) establish the correlation between the profiles in both positions. It is also worth clarifying that this measurement campaign was designed for the purpose of power performance measurement according to [2], and not for research purposes.

Data from both meteorological masts are sampled at a frequency of 1Hz, post processed to 10-minute average statistics, and stored in a datalogger. Data are filtered out according to the following criteria:

- Failure of the measurement equipment due to, for example, icing (filtered out by Temperature<2ºC) or loss of power supply.
- Reference wind speed out of the range [4,16) m/s

Once the flow correction factors ($\alpha_j$) are obtained for all 10º-width sectors within the measurement sector, the following three conditions are checked (following the reference standard) and the measurement sector is re-adjusted according to them. The resulting flow correction factors and measurement sector must fulfil that: 1) there is certain minimum amount of site calibration data in a given direction bin, 2) the flow correction factors don't change too abruptly from one sector to another, 3) the flow correction factors converge to their mean value. Taking these considerations into account, the final measurement sector to be used in the power curve phase is [115º,135º) and [225º,305º).

For the sake of confidentiality, the resulting flow correction factors and their associated uncertainty are not shown here. The obtained flow correction factors fulfil satisfactorily the consistency test performed using power curve data [2, Annex C].

# 6. Power curve

The power curve measurement is performed from 22/4/2009 to 2/8/2009. During this period the lidar is deployed at 12m distance from the reference mast, in the South-West direction (Figure 5).

**Figure 5:** *Position of lidar relative to reference mast and wind turbine under test.*

Data from the meteorological mast and the wind turbine are sampled at a frequency of 1Hz, post processed to 10-minute average statistics, and stored in the datalogger. Data acquired by the

ZephIR is also processed to 10-minute statistics. A database is created with simultaneous data from wind turbine, meteorological mast instruments and lidar data.

Data are filtered out from the database according to the following criteria:

- External conditions, different from wind speed, out of the operating range of the wind turbine.
- Wind turbine stopped in a fault condition. (Detected by means of an "Availability" signal provided by the manufacturer).
- Failure of the measurement equipment due to, for example, icing (filtered out when Temperature<2ºC).
- Wind direction out of the ranges [115º,135º) and [225º,305º).
- Lidar quality filters [1]:
    - Points in Fit: PiF ≥ 35
    - Number of packets in 10min. average: PiA ≥ 50
    - "Turbulence parameter"<0.08
    - Note: In this period it was not necessary to apply the lidar fog filter (no datasets were suspected of fog/low cloud contamination).

The aim of sections 6.1 and 6.2 is to investigate the effect of wind shear on the power curve, and investigate if lidar wind profile information can help in alleviating its effect. However, wind shear is not the only factor influencing the power output of a wind turbine. Wind veer and turbulence intensity can also lead to significant variations of the output power [7]. For this reason, additional filtering criteria are imposed, in an attempt to prevent the scatter in the power curve linked to turbulence intensity from concealing the effect of wind shear:

Turbulence Intensity < 10% and Reference Wind Speed ≥ 6 m/s.

Note that the turbulence filter is only for the purpose of this study. In the standard power performance measurement such a filter should not be applied. Investigating the (significant) effect of turbulence is not in the scope of this work.

No additional filter is applied for wind veer since extreme veer events are not observed in the remaining dataset.

Figure 6 presents the comparison between the wind speed measured by the lidar at hub height and the wind speed measured by the top-mounted cup anemometer in the reference mast, after all the previous filters have been applied:

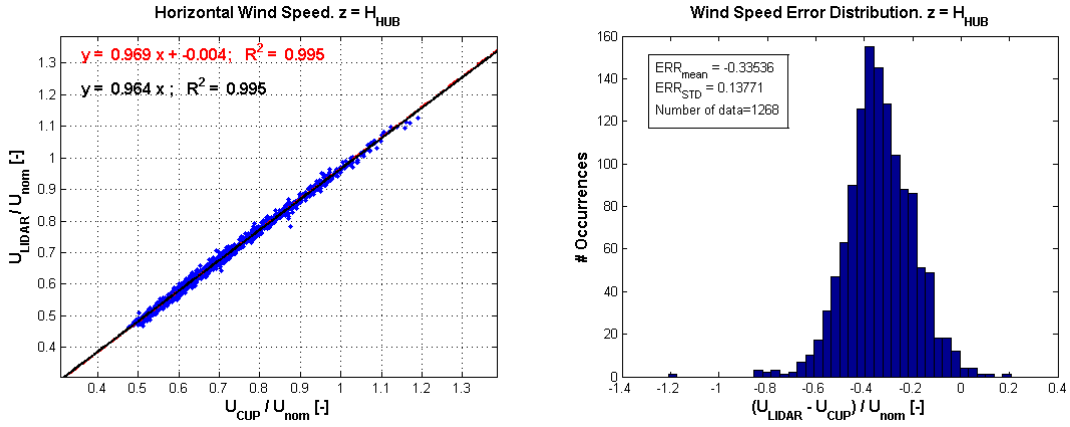


**Figure 6:** *Left: lidar to cup wind speed comparison at $H_{HUB}$. Right: histogram of the (normalized) error distribution.*

Note that there is an overall underestimation of the wind speed measured by the lidar, with respect to the cup wind speed. The investigation of sources for this discrepancy, and the dependence of the wind speed error ($U_{LIDAR}$-$U_{CUP}$) with wind direction, are detailed in [1].

## 6.1 Effect of wind shear on the power curve

As a first step, a classification of the wind profiles measured by the lidar, at the reference mast position, is carried out. This classification is performed based on two parameters: the shear exponent (α) and the residual value (RES).

The wind speeds measured by the lidar at five different heights (4.3) are fitted to the power law model:

$$U_{fit}(z) = U(z_{hub}) \cdot \left( \frac{z}{z_{hub}} \right)^{\alpha} \qquad (1)$$

Where $z_{hub}$ is the hub height of the wind turbine, U is the wind speed, z is the height (a.g.l.), and α is the shear exponent. This model is used because is simple and is widely used by the wind industry to quantify wind shear. Nevertheless, not all wind profiles would be well described by this power law. For this reason, the residual of the fit to the power law is computed using a similar definition to the one proposed in [3]:

$$RES = \frac{\sqrt{\sum_i \left( U_{fit,i} - U_i \right)^2}}{5} \qquad (2)$$

Where i=1..5; $U_i$ is the wind speed measured by the lidar at height $z_i$, and $U_{fit,i}$ is the wind speed value given by the power-law fitting function at height $z_i$. In other words, the parameter "RES" is an estimator of the goodness of the fit to the power law. This means, the RES parameter quantifies how well the profiles are described by the power law.

To obtain the power curve, it is necessary to:

- Correct wind speed data collected by the reference mast with the flow correction factors obtained from the site calibration.
- Correct atmospheric pressure following the standard ISO 2533, for the case of a pressure sensor installed a height different from hub height.
- Apply a normalization to the (corrected) wind speed, according to:

$$V_n = V_{10\,\min} \left( \frac{\rho_{10\,\min}}{\rho_0} \right)^{1/3} \qquad (3)$$

Where:
$V_n$ is the normalized wind speed;
$V_{10min}$ is the measured wind speed averaged over 10 min, corrected by the flow correction factors from site calibration;
$\rho_0$ is the reference air density (average of the measured air density data at the test site during periods of valid data collection);
$\rho_{10min}$ is the 10 min averaged air density;

Figure 7 and Figure 8 present scatter power curves at the site air density, where the datasets are grouped based on different values of α and RES respectively, according to the profile classification described above.

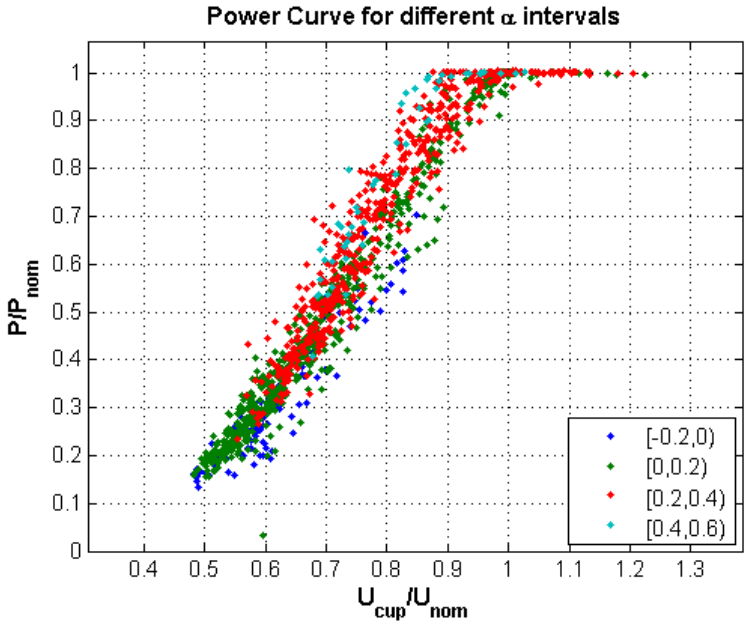


**Figure 7:** *Power curve scatter plots obtained for different values of the shear exponent, using the cup wind speed at hub height.*

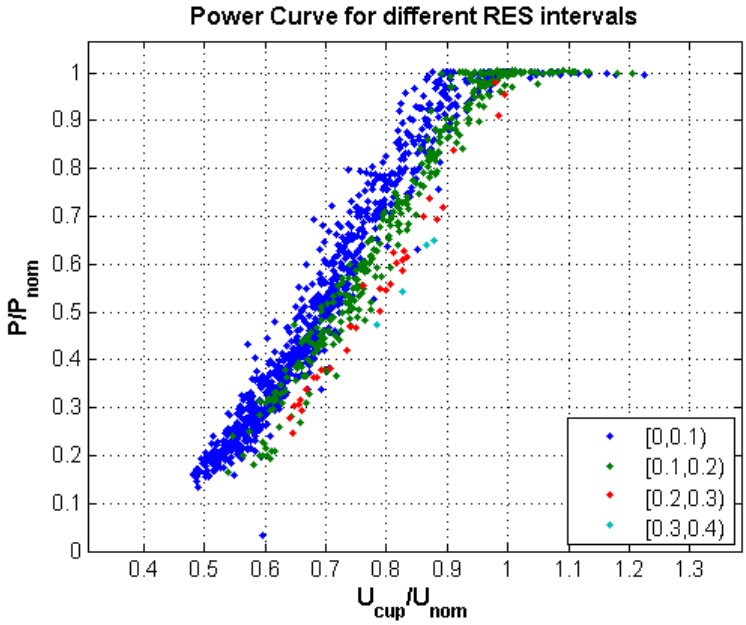


**Figure 8:** *Power curve scatter plots obtained for different values of the RES parameter, using the cup wind speed at hub height.*

From previous graphs, we can see that the wind profile, and in particular its shape (RES), affects the power output:

- Profiles that are well defined by the power law (low RES), correspond to higher power values, for a given reference wind speed.
- Profiles that are not well defined by the power law (high values of RES), which could be considered “extreme profiles”, correspond to a lower power output.

## 6.2 Equivalent wind speed analysis

Next step is to adapt the equivalent wind speed method from [3] to this case, using the lidar wind speed measurements obtained at different heights at the reference mast position. The goal is to produce a power curve in terms of (P,Ueq), being P the power output, and Ueq an equivalent wind speed averaged across the rotor swept area. The aim is to check if such a curve displays less scatter than the power curve presented in Figure 8.

Two different definitions for the equivalent wind speed, Ueq, have been tried:

$$Ueq_1 = \left( \sum_i U_i^{\,3} \frac{A_i}{A} \right)^{1/3} \qquad (4)$$

$$Ueq_2 = \frac{1}{A} \sum_i U_i \cdot A_i \qquad (5)$$

Where $U_i$ (with i=1...5) is the wind speed at height $H_i$, and $A_i$ is the portion of rotor area corresponding to $H_i$, as illustrated in Figure 9. Both definitions have produced very similar results, so for the sake of clarity only the results obtained with $Ueq_1$ are displayed in the following points.

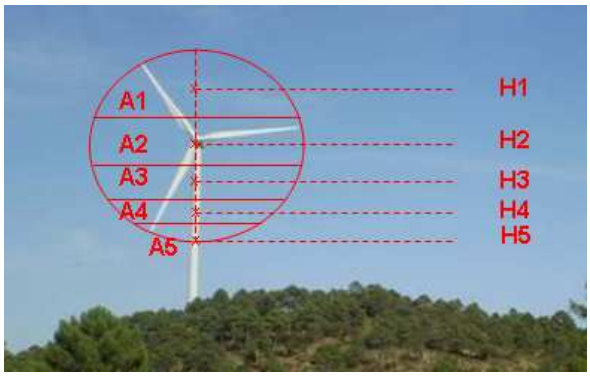


**Figure 9:** *Lidar measurement heights (H1..H5) and their corresponding sections of rotor area (A1..A5).*

It must be pointed out that the $U_i$ in eq.4 and eq.5 are the wind speeds incident in the wind turbine rotor. The difficulty of applying the equivalent wind speed method to a complex terrain case is how to correlate the wind profile measured by the lidar (located at a 2.5 rotor diameter distance from the wind turbine) to the wind profile at the turbine position.

### 6.2.1 "Non-shifted" lidar profiles

In this first approach, two assumptions are made:

- The same flow correction factors ($\alpha_j$) obtained from site calibration with cups can be applied to lidar hub height wind speeds. We know that this is not the case, because as Figure 6 shows, the lidar wind speed at hub height is smaller than the cup speed at that height, and consequently, different (higher) flow correction factors should be used.

- The $\alpha_j$ factors obtained for hub height wind speeds can be applied to all heights. That means: the shape of the profile is maintained from the reference mast position to the wind turbine position. This may not be the case in complex terrain; however this is not taken into account by the standard site calibration.

Thus, the $\alpha_j$ factors are applied to lidar wind speed measurements, the equivalent wind speed is calculated according to eq.4, and normalized to the site air density. The resulting power curves using cup wind speed at hub height, and the lidar equivalent wind speed, are shown in Figure 10 and Figure 11 respectively.

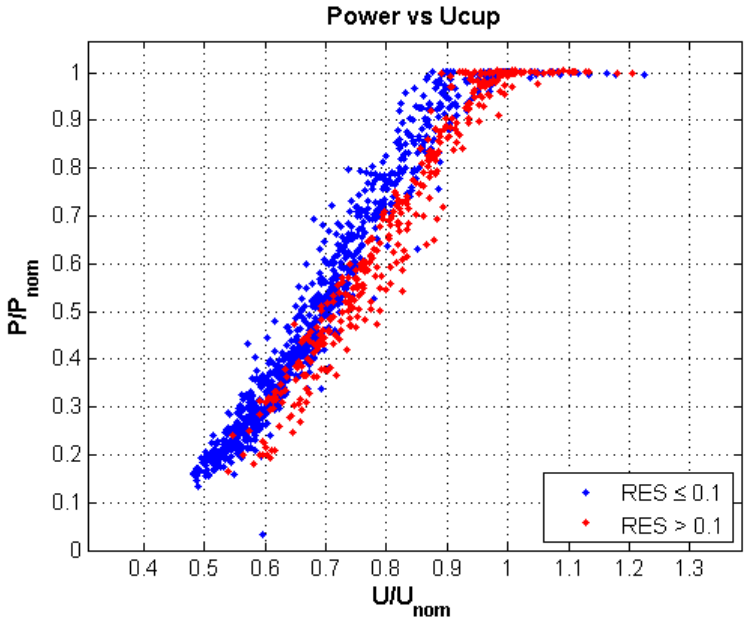


**Figure 10:** *Power curve scatter plot obtained with the wind speed measured by the cup anemometer at hub height.*

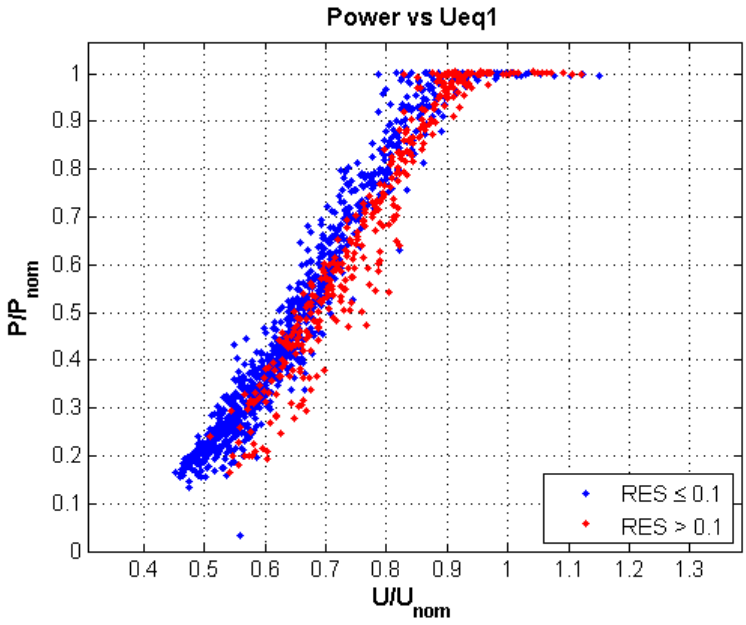


**Figure 11:** *Power curve scatter plot obtained with the lidar equivalent wind speed.*

In both graphs the data set is divided into two groups: 1) speed profiles with a shape close to the power law model (RES≤0.1); 2) speed profiles that are not well described by the power law (RES>0.1). Comparing the two graphs, there is still a significant scatter in Figure 11; however the two groups of data become closer (i.e. the scatter of the curve is reduced) for the higher wind speeds.

In order to better quantify the scatter in both cases, a definition of the power curve scatter relative to the mean power curve is made, according to [3]:

First, the mean power curve is calculated, using the method of bins. Then, the scatter is quantified as the residual error per each line segment as:

$$RES_{POWER} = \frac{\sqrt{\sum_{n}\left(P_{fit}^{i}(v_{i,n}) - P_{i,n}\right)^2}}{N} \qquad (6)$$

Where:

n=1...N

N: number of data in the $i^{th}$ segment

$P_{i,n}$ is the measured power for the $n^{th}$ point in the $i^{th}$ segment

$V_{i,n}$ is the measured wind speed for the $n^{th}$ point in the $i^{th}$ segment

$P^{i}_{fit}$ is the line equation of the $i^{th}$ segment, given by:

$$P_{fit}^{i} = \left(\frac{P_{Pi+1} - P_i}{v_{i+1} - v_i}\right)\cdot v + \left(P_{i+1} - \frac{P_{i+1} - P_i}{v_{i+1} - v_i}\cdot v_{i+1}\right) \qquad (7)$$

Where $(v_i,P_i)$ and $(v_{i+1},P_{i+1})$ are the two ends of the segment. They are, respectively, the mean wind speed and mean power in bin “i” of the power curve, and the mean wind speed and mean power in bin “i+1” of the power curve.

Figure 12 shows the mean power curves for different reference wind speeds: cup wind speed at hub height, lidar wind speed at hub height, and lidar equivalent wind speed. Only the fragment of interest is displayed (the range of wind speeds which present the highest scatter in Figure 10 and Figure 11) – wind speeds between $0.45U_{nom}$ and $U_{nom}$. Both the curve obtained with the lidar wind speed at hub height, and the equivalent wind speed, are displaced to the left compared to the curve obtained with the cup anemometer. They are a consequence of: a) in both cases, the underestimation of wind speed made by lidar at hub height, as seen from Figure 6; b) in the case of the equivalent wind speed, probably caused too, and further left-shifted, by the underestimation of wind speeds by lidar at other heights [1].

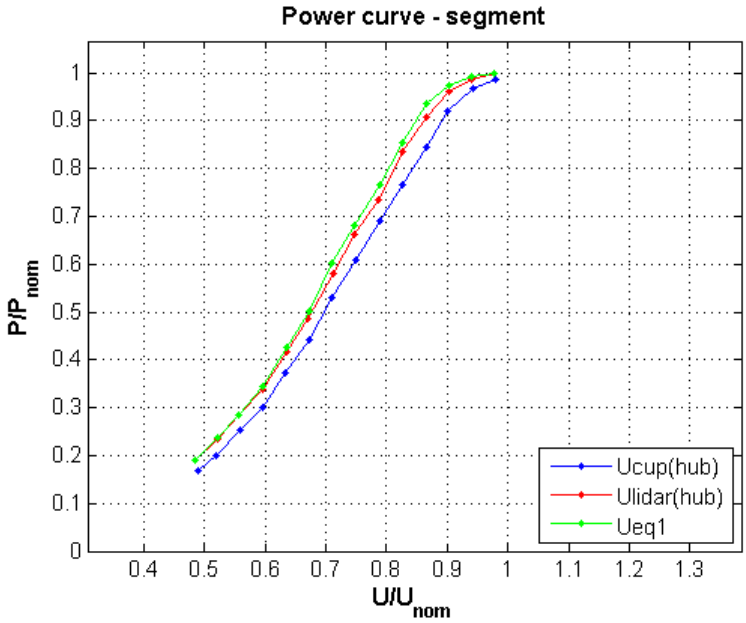


**Figure 12:** *Binned power curve for three reference wind speeds: cup at hub height (blue), lidar at hub height (red) and equivalent wind speed (green).*

Finally, the residual errors in power curve per bin are displayed in Figure 13. It shows that the use of the equivalent wind speed reduces the scatter of the curve only for wind speeds greater than $0.65U_{nom}$. Note that for lower wind speeds there are very few profiles with RES>0.1 (Figure 8), thus it is not surprising that the method does not present an improvement in those bins.

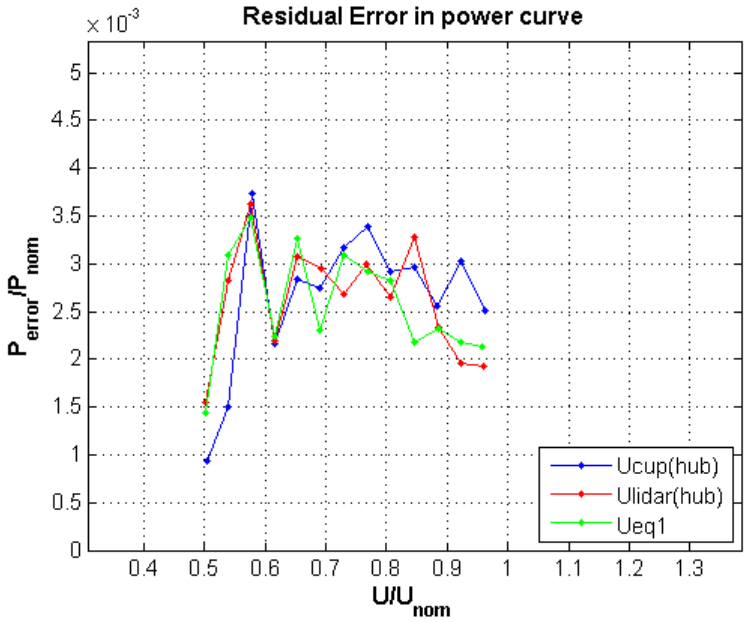


**Figure 13:** *Mean residual error in power curve for three reference wind speeds: cup at hub height (blue), lidar at hub height (red) and equivalent wind speed (green).*

### 6.2.2 "Shifted" lidar profiles

In order to avoid the first of the assumptions in previous point, the wind profile is "corrected " or "shifted", so that the lidar wind speed at hub height equals the cup wind speed at hub height (Figure 14). This would imply that the lidar wind speed error ($U_{LIDAR}$-$U_{CUP}$) is constant with height. In the lidar to mast correlation study performed in D6.6.2 [1], the mean of the lidar wind speed error was found to be different at different heights, although a systematic increase or decrease of the mean error with height was not observed. So, the procedure of shifting the lidar profile is yet another approximation to deal with the limitation of not having a lidar during site calibration.

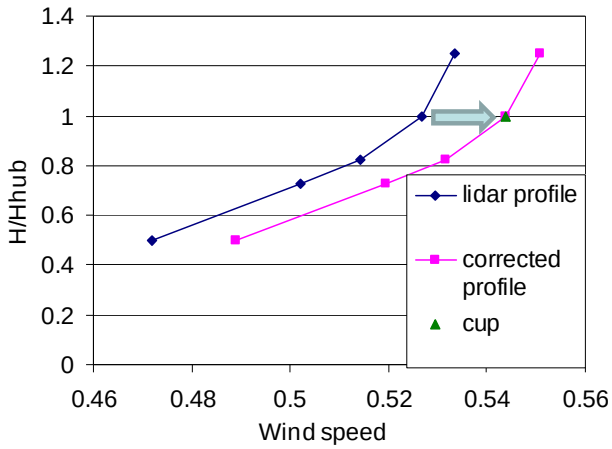


**Figure 14:** *Example of lidar profile shift in one 10-min. Triangle: cup measurement. Diamonds: lidar measured profile. Squares: lidar shifted profile.*

Figure 15 and Figure 16 show, respectively, the resulting mean power curve and the mean residuals obtained using the cup hub height wind speed and the equivalent wind speed obtained from the shifted lidar profile. As seen in Figure 16, shifting the lidar profile before calculating the equivalent wind speed doesn't present an improvement, since there is not a significant reduction in the residual error in the power curve.

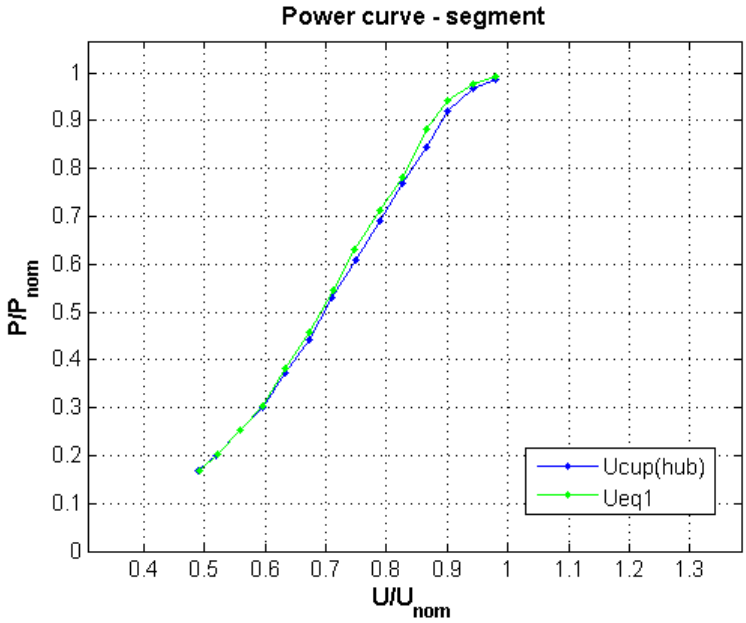


**Figure 15:** *Binned power curve for three reference wind speeds: cup at hub height (blue) and equivalent wind speed (green).*

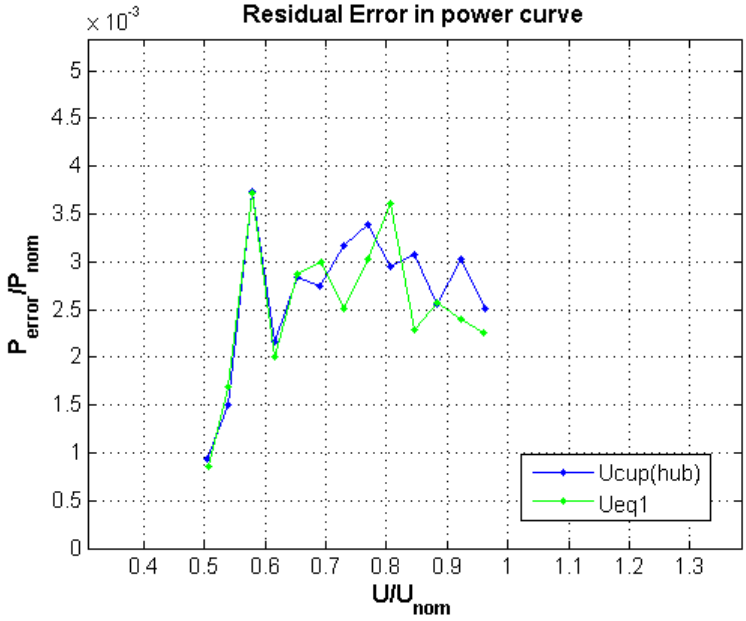


**Figure 16:** *Mean residual error in power curve for two reference wind speeds: cup at hub height (blue) and equivalent wind speed obtained from shifted lidar profile (green).*

### 6.2.3 Simulation of lidar-specific flow correction factors

In D6.6.2, numerical models (Wasp Engineering [8] and CFDWind2.0 [9]) were used to obtain the ratio, per wind direction sector, between the wind speed measured by the lidar at a given height, and the wind speed at that height at the lidar position. A similar approach is proposed here, to cope with the lack of wind speed profile data from the experimental site calibration.

For simplicity, and since the lidar is very close to the reference mast (12m distance), in the following the lidar and mast position are assumed to be the same, which is referred to as the "reference position".

The flow models can be used to obtain the following site calibration "lidar-specific" flow corrections factors, $\beta_{j,i}$:

$$\beta_{j,i} = \frac{U_{WTG,j}(z_i)}{U_{LIDAR,j}(z_i)} \qquad (8)$$

Where:
i=1..5;
$z_i$ are the heights of interest: $0.5H_{HUB}$, $0.73H_{HUB}$, $0.83H_{HUB}$, $H_{HUB}$ and $1.25H_{HUB}$.
$U_{WTG,j}(z_i)$ is the horizontal wind speed at the wind turbine position at height $z_i$, obtained from the simulations in the $j^{th}$ direction sector .
$U_{LIDAR,j}(z_i)$ is the lidar horizontal wind speed at the reference position, at height $z_i$, obtained from the simulations in the $j^{th}$ direction sector.

The lidar horizontal wind speed $U_{LIDAR,j}(z_i)$, obtained from the simulations, is computed from a series of radial wind speeds (projections of the simulated wind vector, along different trajectories of the laser beam, in different points in the lidar circle of scan), at the given height.

These $\beta_{j,i}$ factors could then be applied to the wind speed profile measured by the lidar at the reference position, and they would correct simultaneously for:

- any possible direction dependent error in the speed profile measured by the lidar
- the possible change between the speed profile at the reference position and the speed profile at the wind turbine position.

Once this correction is made, the equivalent wind speed would be calculated from the corrected profile, and finally normalized to the reference air density. The resulting (equivalent) wind speed would then be used as the reference wind speed (abscissa) of the power curve.

In this case, the $\beta_{j,i}$ factors are calculated for 10º-direction bins inside the sector [225º,305º) with both models. The measurement sector has been reduced only for demonstration purposes, in order to reduce the duration and the preparation of the CFD simulations, due to the time limitation mentioned in D6.6.2.

The results obtained after applying both sets of factors are inconclusive, for the time being. The reasons are that: 1) there are some significant differences between the sets of $\beta_{j,i}$ obtained with both models; 2) the consistency of both sets of factors is difficult to assess without experimental data from at least one height (measurements of $U_{LIDAR}(H_{hub})$ and $U_{WTG}(H_{hub})$).

Two checks are made, using the available experimental data, in attempt to identify which set of factors produces more plausible results:

- Obtain with the models the ratios (at hub height) between the wind speeds at the turbine position and the wind speeds at the reference position, for different direction sectors ($\alpha'_j$) and compare them to the ratios from the experimental site calibration ($\alpha_j$):

$$\alpha'_j = \left( \frac{U_{WTG,j}(H_{hub})}{U_{REF,j}(H_{hub})} \right)_{simulations}$$
$$\alpha_j = \left( \overline{\left( \frac{U_{WTG}(H_{hub})}{U_{REF}(H_{hub})} \right)_j} \right)_{experimental} \quad (9)$$

Where:

$U_{WTG,j}(H_{hub})$ is the horizontal wind speed at the wind turbine position at hub height, obtained from the simulations in the $j^{th}$ direction sector.

$U_{REF,j}(H_{hub})$ is the horizontal wind speed at the reference position at hub height, obtained from the simulations in the $j^{th}$ direction sector.

$\overline{\left( \frac{U_{WTG}(H_{hub})}{U_{REF}(H_{hub})} \right)_j}$ is the measured mean wind speed ratio between the cup anemometer at hub height in the turbine position and the cup anemometer in the reference mast at hub height.

- Compare $\beta_{j,4}$ (lidar flow correction factors at hub height) to the products:

$$\alpha_j \cdot \overline{\left( \frac{U_{REF}(H_{hub})}{U_{LIDAR}(H_{hub})} \right)_j} \quad (10)$$

Where $\overline{\left( \frac{U_{REF}(H_{hub})}{U_{LIDAR}(H_{hub})} \right)_j}$ is the measured mean ratio between the cup and lidar wind speed in the $j^{th}$ direction sector at hub height.

In both cases, the level of agreement between models and experimental results varies for the different wind direction sectors. As a consequence, no conclusion has been reached of which of the models is more suitable for this application. It remains for further study:

- To quantify the impact that the uncertainty associated to the "lidar-specific" flow corrections factors, obtained by simulations, has in the equivalent-wind speed power curve.
- To further analyse and filter the dataset.
- Possibly adjust the simulations.
- Investigate if a consistency test of the "lidar-specific" flow corrections factors can be carried out using power curve data.

# 7. Conclusions and further work

This report has summarized the results of an approach to the application of the equivalent wind speed method for power performance measurements, in a complex terrain case. The work has focused on investigating whether the use of the equivalent wind speed definition (obtained from the wind profile measured by the lidar) produces a reduction in the power curve scatter, in comparison to the standard power curve where only hub height wind speed is used as the reference wind speed.

However, in this case, the application of the equivalent wind speed method is constrained by not having enough experimental data to:

- check if there are significant changes between the profiles at the lidar/mast position and at the wind turbine position.
- establish the correlation between the profiles in both positions.

Due to this constraint, the results obtained in 6.2.1 and 6.2.2 have to be taken with caution, since some assumptions had to be made to cope with the lack of profile information during site calibration. The results obtained in both cases can be summarized, respectively, as follows:

- the use of the equivalent wind speed obtained from lidar measurements reduced the scatter of the power curve in the higher wind speed bins. Nevertheless, this reduction is small.
- shifting the lidar profile, based on cup measurements at hub height, doesn't produce an overall improvement, in terms of reduction of the power curve scatter. It only allows correlating, to a small extent, the wind profile at the reference position (position of lidar and mast) to the wind turbine position, by means of the flow correction factors obtained in the standard experimental site calibration. However, it is arguable whether the shift applied at hub height could be applied to the rest of the heights.

It has been identified that, in the use of lidars to obtain equivalent wind speeds for power curves in complex terrain, two sources of uncertainty need to be addressed:

- any possible direction dependent error in the speed profile measured by the lidar
- the possible change between the speed profile at the reference position and the speed profile at the wind turbine position.

An attempt at using flow modelling to correct for the two previous factors has been described in the report. Few conclusions could be drawn from the work carried out up to date, once again due to the lack of experimental wind profile data to corroborate the results of the models. However, further work on this subject is still needed.

The limitations encountered in this campaign highlight the necessity to have a good experimental characterization of wind profiles in site calibrations for power performance measurements in complex terrain, especially if the equivalent wind speed method is to be applied. More experimental work is needed to find optimal campaign designs for such a characterization (in terms of number of lidars involved during site calibration or masts configurations), in order to reduce the uncertainty of the wind profile measurements. Some work is being carried out in this line within the SafeWind Project [10], in work package 2, where some output is expected regarding the experimental determination of equivalent wind speeds in flat and complex terrains.

# 8. Acknowledgements

The author would like to express her gratitude to Gustavo Rodríguez and Sogepyme S.A. for allowing this campaign to be carried out and for the assistance provided during it.

This work would have not been possible without the field support of the technicians and the collaboration and advice from the power curve engineers (Óscar Elizalde, Ignacio Navarro, Gabriel Alzueta), from the Field Tests area at CENER's Wind Turbine Test Laboratories.

Many thanks to Rozenn Wagner and Mike Courtney for their help.

The previously mentioned persons are not responsible of any possible errors or omissions in this report.

# 9. References

1. P. Gómez "UPWIND D6.6.2 Report – Measurements in complex terrain using a lidar". 2011.
2. IEC 61400-12-1 "Power performance measurements of electricity producing wind turbines", Edition 2005.
3. R. Wagner "Accounting for the speed shear in wind turbine power performance measurement". Risø-PhD-58(EN). 2010.
4. UNE-EN ISO/IEC 17025:2000 "Requisitos generales relativos a la competencia de los laboratorios de ensayo y calibración".
5. MEASNET "Cup Anemometer Calibration Procedure Version 2". October 2009.
6. T.F. Pedersen, J.-Å. Dahlberg, P. Busche "ACCUWIND – Classification of five anemometers according to IEC61400-12-1". 2006.
7. I. Antoniou, S.M. Pedersen "Influence of turbulence, wind shear and low-level jets on the power curve and the AEP of a wind turbine". EWEC 2009 proceedings.
8. F. Bingöl, J. Mann. "Lidar performance estimation script for WAsP Engineering". Risø-R-1664(EN). 2008.
9. J. Sanz, D. Cabezón, S. Lozano, I. Martí "Parameterization of the atmospheric boundary layer for offshore wind resource assessment with a limited length-scale k-ε model". EWEC 2009 proceedings.
10. SafeWind Project: "Multi-scale data assimilation, advanced wind modelling and forecasting with emphasis to extreme weather situations for a secure large-scale wind power integration". FP7-ENERGY-2007-1-RTD. http://www.safewind.eu/